REPORT DOCUMENTATION PAGE	Form Approved OMB NO. 0704-0188

The public reporting burden for this collection of information is estimated to average 1 hour per response, including the time for reviewing instructions, searching existing data sources, gathering and maintaining the data needed, and completing and reviewing the collection of information. Send comments regarding this burden estimate or any other aspect of this collection of information, including suggesstions for reducing this burden, to Washington Headquarters Services, Directorate for Information Operations and Reports, 1215 Jefferson Davis Highway, Suite 1204, Arlington VA, 22202-4302. Respondents should be aware that notwithstanding any other provision of law, no person shall be subject to any oenalty for failing to comply with a collection of information if it does not display a currently valid OMB control number.
PLEASE DO NOT RETURN YOUR FORM TO THE ABOVE ADDRESS.

1. REPORT DATE (DD-MM-YYYY)	2. REPORT TYPE	3. DATES COVERED (From - To)
31-10-2016	Final Report	5-Aug-2013 - 4-Aug-2016

4. TITLE AND SUBTITLE
Final Report: Topological Insulators for Novel Device Applications

5a. CONTRACT NUMBER
W911NF-13-1-0300

5b. GRANT NUMBER

5c. PROGRAM ELEMENT NUMBER
611102

5d. PROJECT NUMBER

5e. TASK NUMBER

5f. WORK UNIT NUMBER

6. AUTHORS
Ki Wook Kim

7. PERFORMING ORGANIZATION NAMES AND ADDRESSES
North Carolina State University
2701 Sullivan Drive
Admin Srvcs III, Box 7514
Raleigh, NC 27695 -7514

8. PERFORMING ORGANIZATION REPORT NUMBER

9. SPONSORING/MONITORING AGENCY NAME(S) AND ADDRESS (ES)
U.S. Army Research Office
P.O. Box 12211
Research Triangle Park, NC 27709-2211

10. SPONSOR/MONITOR'S ACRONYM(S)
ARO

11. SPONSOR/MONITOR'S REPORT NUMBER(S)
61948-EL.9

12. DISTRIBUTION AVAILIBILITY STATEMENT
Approved for Public Release; Distribution Unlimited

13. SUPPLEMENTARY NOTES
The views, opinions and/or findings contained in this report are those of the author(s) and should not contrued as an official Department of the Army position, policy or decision, unless so designated by other documentation.

14. ABSTRACT
This research program theoretically exploited unique characteristics of the topological insulator based structures for highly functional devices for room temperature operation. Utilizing the spin-momentum interlocked nature originating from strong spin-orbit coupling in such materials, the key focus was to achieve electrical control of both degrees of freedom for integration of electronics and magnetics into a single nanoscale system. A number of innovative new concepts were put forth by judiciously employing hybrid structures formed with magnetic materials. Specific applications were pursued in three different areas – multifunctional charge/spin current

15. SUBJECT TERMS
Topological insulators, magnetoelectric effects, spin devices, theoretical modeling

16. SECURITY CLASSIFICATION OF: a. REPORT	b. ABSTRACT	c. THIS PAGE	17. LIMITATION OF ABSTRACT	15. NUMBER OF PAGES	19a. NAME OF RESPONSIBLE PERSON
UU	UU	UU	UU		Ki Wook Kim
					19b. TELEPHONE NUMBER 919-515-5229

Report Title

Final Report: Topological Insulators for Novel Device Applications

ABSTRACT

This research program theoretically exploited unique characteristics of the topological insulator based structures for highly functional devices for room temperature operation. Utilizing the spin-momentum interlocked nature originating from strong spin-orbit coupling in such materials, the key focus was to achieve electrical control of both degrees of freedom for integration of electronics and magnetics into a single nanoscale system. A number of innovative new concepts were put forth by judiciously employing hybrid structures formed with magnetic materials. Specific applications were pursued in three different areas – multifunctional charge/spin current modulation, nonvolatile magnetic switching, and high sensitivity THz/far infrared detection. The investigation encompassed both analysis of fundamental properties of topological insulators and the device modeling. While the basic operating principles of the envisioned devices were explored with the development of physical models, numerical modeling was also adopted to establish concrete designs as well as realistic estimates of performance specifications. The obtained results are expected to have significant potential impacts on room-temperature multi-functional spintronics, integration of magnetism with nanoelectronics, and far infrared sensing technologies.

Enter List of papers submitted or published that acknowledge ARO support from the start of the project to the date of this printing. List the papers, including journal references, in the following categories:

(a) Papers published in peer-reviewed journals (N/A for none)

Received		Paper
07/27/2015	4.00	Xiaopeng Duan, Yuriy G. Semenov, Ki Wook Kim. Spin Logic via Controlled Correlation in Nanomagnet–Dirac-Fermion Heterostructures, PHYSICAL REVIEW Applied, (10 2014): 44003. doi: 10.1103/PhysRevApplied.2.044003
07/27/2015	5.00	Xiaopeng Duan, Xiaodong Li, Yuriy G. Semenov, Ki Wook Kim. Quasi-optical electron transport across a magnetically induced junction on a topological insulator surface, Journal of Applied Physics, (12 2014): 224301. doi: 10.1063/1.4903798
08/13/2014	1.00	Xiaopeng Duan, Xiaodong Li, Ki Wook Kim. Controlling electron propagation on a topological insulator surface via proximity interactions, Physical Review B, (01 2014): 45425. doi: 10.1103/PhysRevB.89.045425
08/13/2014	2.00	Xiaodong Li, Yuriy G. Semenov, Ki Wook Kim. Thin-film topological insulator-ferromagnet heterostructures for terahertz detection, Applied Physics Letters, (02 2014): 61116. doi: 10.1063/1.4865423
08/13/2014	3.00	Yuriy G. Semenov, Xiaopeng Duan, Ki Wook Kim. Voltage-driven magnetic bifurcations in nanomagnet–topological insulator heterostructures, Physical Review B, (05 2014): 201405. doi: 10.1103/PhysRevB.89.201405

TOTAL: **5**

Number of Papers published in peer-reviewed journals:

(b) Papers published in non-peer-reviewed journals (N/A for none)

Received Paper

TOTAL:

Number of Papers published in non peer-reviewed journals:

(c) Presentations

X. Li, X. Duan, and K. W. Kim, "Dirac Fermion Wave Guiding on Topological Insulator Surfaces via Proximity Interactions," presented at SPINTECH-VII (August, 2013, Chicago, Illinois).

X. Duan, Y. G. Semenov, and K. W. Kim, "Dynamics of Magnetization Switch in TI/FM Structures for All Spin Logic Applications," presented at SPINTECH-VII (August, 2013, Chicago, Illinois).

Y. G. Semenov, X. Duan, and K. W. Kim, "Voltage Driven Magnetic Bifurcations in Nanomagnet-Topological Insulator Composite Structures," presented at the March Meeting of the American Physical Society (March, 2014, Denver, Colorado); Bull. Am. Phys. Soc. 58, D41.00011 (2014).

X. Duan, Y. G. Semenov, and K. W. Kim, "Zero Field Conductance Singularity in Two Terminal Ferromagnet-Topological Insulator Device," presented at the March Meeting of the American Physical Society (March, 2014, Denver, Colorado); Bull. Am. Phys. Soc. 58, D41.00015 (2014).

X. Duan, X. Li, Y. G. Semenov, and K. W. Kim, "Proposal of a Topological Insulator Based Magnetoelectric Transistor," presented at the 72nd Annual Device Research Conference (June, 2014, Santa Barbara, California).

A. Barrette, C. Mai, Y. Yu, Y. Semenov, Z. Jin, K. W. Kim, L. Cao, and K. Gundogdu, "Ultrafast Valley Relaxation Dynamics in Single Layer Semiconductors," presented at SPIE Optical Engineering + Applications – Ultrafast Nonlinear Imaging and Spectroscopy II (August, 2014, San Diego, California).

Z. Jin, Y.-F. Lee, S. Nori, K. W. Kim, J. Narayan, and D. Kumar, "Strain Induced Room Temperature Ferromagnetism in Epitaxial Magnesium Oxide Thin Films," presented at the 2015 Materials Research Society Spring Meeting (April, 2015, San Francisco, California).

Zhenghe Jin, Raj Kumar, Frank Hunte, Jay Narayan, and Ki Wook Kim, "Microstructural and Magneto-Transport Characterization of Bi_2 (Se_xTe_1-x)3 Topological Insulator Thin Films Grown by Pulsed Laser Deposition Method," presented at the March Meeting of the American Physical Society (March, 2016, Baltimore, Maryland); Bull. Am. Phys. Soc. 61, T1.00086 (2016).

Xi-Lai Li, Xiaopeng Duan, Yuriy G. Semenov, and Ki Wook Kim, "Electrically Controlled Switching of Antiferromagnets via Proximity Interaction Induced by Topological Insulator," presented at the 74th Annual Device Research Conference (June, 2016, Newark, Delaware), Conf. Digest, pp. 231-232.

Number of Presentations: 9.00

Non Peer-Reviewed Conference Proceeding publications (other than abstracts):

Received Paper

TOTAL:

Number of Non Peer-Reviewed Conference Proceeding publications (other than abstracts):

Peer-Reviewed Conference Proceeding publications (other than abstracts):

Received Paper

TOTAL:

Number of Peer-Reviewed Conference Proceeding publications (other than abstracts):

(d) Manuscripts

Received Paper

TOTAL:

Number of Manuscripts:

Books

Received Book

TOTAL:

Received	Book Chapter

TOTAL:

Patents Submitted

Patents Awarded

Awards

Ki Wook Kim, Fellow, American Physical Society, 2015

Graduate Students

NAME	PERCENT_SUPPORTED	Discipline
Xiaopeng Duan	0.40	
Xi-Lai Li	0.50	
Zhenghe Jin	0.10	
FTE Equivalent:	**1.00**	
Total Number:	**3**	

Names of Post Doctorates

NAME	PERCENT_SUPPORTED
Yuriy Semenov	0.25
FTE Equivalent:	**0.25**
Total Number:	**1**

Names of Faculty Supported

NAME	PERCENT_SUPPORTED	National Academy Member
Ki Wook Kim	0.07	
FTE Equivalent:	**0.07**	
Total Number:	**1**	

Names of Under Graduate students supported

NAME	PERCENT_SUPPORTED
FTE Equivalent:	
Total Number:	

Student Metrics

This section only applies to graduating undergraduates supported by this agreement in this reporting period

The number of undergraduates funded by this agreement who graduated during this period: 0.00

The number of undergraduates funded by this agreement who graduated during this period with a degree in science, mathematics, engineering, or technology fields:...... 0.00

The number of undergraduates funded by your agreement who graduated during this period and will continue to pursue a graduate or Ph.D. degree in science, mathematics, engineering, or technology fields:...... 0.00

Number of graduating undergraduates who achieved a 3.5 GPA to 4.0 (4.0 max scale):...... 0.00

Number of graduating undergraduates funded by a DoD funded Center of Excellence grant for Education, Research and Engineering:...... 0.00

The number of undergraduates funded by your agreement who graduated during this period and intend to work for the Department of Defense 0.00

The number of undergraduates funded by your agreement who graduated during this period and will receive scholarships or fellowships for further studies in science, mathematics, engineering or technology fields:...... 0.00

Names of Personnel receiving masters degrees

NAME

Total Number:

Names of personnel receiving PHDs

NAME

Xiaopeng Duan

Total Number: **1**

Names of other research staff

NAME	PERCENT_SUPPORTED
FTE Equivalent:	
Total Number:	

Sub Contractors (DD882)

Inventions (DD882)

Scientific Progress

See Attachment

Technology Transfer

3. Scientific Progress and Accomplishments

This research project pursued theoretical understanding and exploration of the unique characteristics of topological insulator based structures for potential device applications via the strong correlation with magnetic materials. Highlights include new device concepts for high sensitivity THz/far infrared detection, energy efficient magnetic switching/persistent oscillations, and multifunctional charge/spin current modulation. The investigation established not only the basic design and the operating principles but also the comprehensive performance estimate at the device level as well as at a simple circuit level, elucidating the potential advantages of the proposed concepts over the conventional counterparts. A brief description of the highlights is given below.

A. High Sensitivity Detection of Long Wave Length Photons

We explored the symmetry-breaking band modification in a topological insulator (TI) structure for the possibility of long-wavelength photo-detection at room temperature. More specifically, we utilized a TI in the thin-film form to induce strong coupling between the two surface states (i.e., top and bottom) that is in addition to the interaction with a proximate magnetic layer (see Fig. 1; right panel). The interplay of these two effects offers a wide parameter space in tailoring the absorption characteristics with an effective control. Further, separation of the optically active surface (i.e., top) from the interface for magnetic interactions (i.e., bottom) enables efficient coupling to the incoming radiation without unnecessary hindrance. Numerical calculations illustrated the unique patterns in the distribution of optically excited carriers that depend sensitively on the frequency of the incoming light (Fig. 1; left panel). At low temperatures (e.g., 4 K), electron transition to the states below the Fermi level is suppressed as they are occupied. Correspondingly, the generation rate below the equipotential line of 0.1 eV (i.e., Fermi level) is nearly zero and the excitation patterns are generally tight with little/no thermal broadening [Figs. 1(a,c,e)]. At elevated temperatures, the pictures deviate from the ideal description due to the thermal broadening [Figs. 1(b,d,f)]. Nevertheless, the asymmetric excitation pattern between $+k_x$ and $-k_x$ remains. This effect results in the generation of strong nonzero photocurrent, leading potentially to room-temperature detection of far-infrared/THz radiation with the advantage of low noise and fast response. A subsequent analysis revealed that the photon energy as low as a few meV (i.e., in the THz frequencies) is indeed accessible by the proposed photogalvanic effect in the thin-film TI structure. The ease of frequency tuning by an external electrical bias offers an added versatility in the realistic implementation.

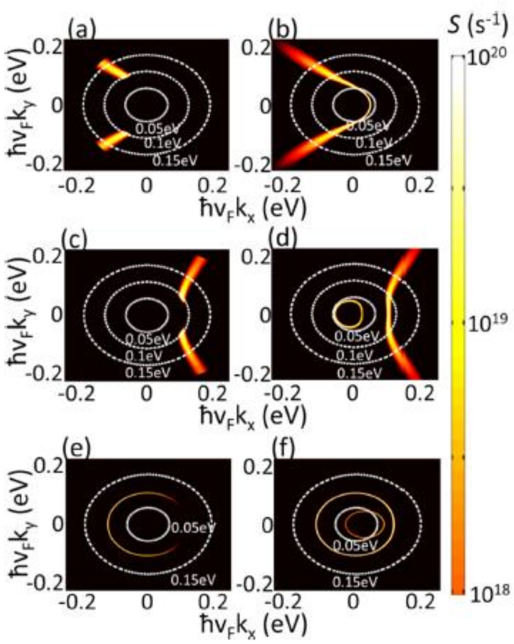

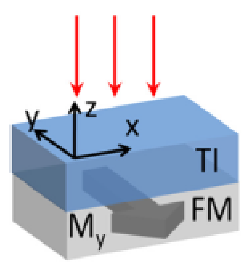

Figure 1: (Right) Proposed TI-ferromagnet (FM) hetero-structure for THz/far-IR detection. (Left) Calculated electron generation rates for the top-surface conduction band plotted in the 2D k-space. The assumed photon energies and the temperatures are: (a) $\hbar\omega$=70 meV, T=4 K; (b) $\hbar\omega$=70 meV, T=300 K; (c) $\hbar\omega$=120 meV, T=4 K; (d) $\hbar\omega$=120 meV, T=300 K; (e) $\hbar\omega$=204 meV, T=4 K; (f) $\hbar\omega$=204 meV, T=300 K. The dashed circles denote the equipotential lines for the electronic bands on the top surface. The Fermi level is at 0.1 eV.

B. Low-Power Magnetic Switching

(a) Electrically controlled all-spin based logic platform:

We explored a low-power all-spin logic platform whose functionality is inspired by the unique properties of the TIs. Figure 2(a) illustrates the basic building component of the system. As shown, each cell (or device) is envisioned with a FM-TI stack placed on top of the graphene channel. In addition, top and bottom gate electrodes (which are separated from the active region by a thin dielectric, respectively) are added for the control clocks. The interface between the FM and the TI is used to locally control the magnet, while that between the FM and the graphene channel supports the means of interconnect. More specifically, the information is encoded in the magnetization orientation of the magnet (FM), which is then transferred to the electron spin polarization in the graphene layer for dissemination. A functional combination of these two interfaces with the information-carrying FM in the middle enables to meet the two major requirements of logic device design: (i) manipulation of the desired information state variable and (ii) robust propagation of information.

In the operation of a specific cell (i.e., single-cell operation), a scheme based on Bennett clocking was developed by taking advantage of the strong correlation between the TI and the FM. Our earlier investigation theoretically demonstrated that a 90° rotation of magnetization between the in-plane and the out-of-plane orientations can be induced by simply controlling the Fermi level of the TI surface states (i.e., the top gate bias). As graphically shown in Fig. 2(b), the key is the reliable signal torque that determines the final state once the 90° rotation puts the magnetization to the metastable out-of-plane direction (the Null state). The signal pulse is applied in concert with the withdrawal of the top gate bias in the Bennet clocking method to minimize the required strength (the Active state). Following a detailed analysis and design, this crucial step was achieved with high fidelity, leading to the deterministic 180° switching (thus, the encoding of logic "1" and "0"). Figure 2(c) provides a numerical demonstration of two successive 180° switching operations.

For the logic function, it is critical to go beyond the single-cell operation where robust propagation of information from the upstream cells to the downstream cells is essential as mentioned above. For an efficient spin logic implementation, the preferred scheme is that the information is transferred in the form of electron spin polarization to avoid the intrinsically inefficient conversion to the electric current. One constraint, however, is the limited distance for reliable signals. Even though graphene enjoys weak spin relaxation and is an ideal choice for the spin channel or interconnect, its characteristic relaxation length is nevertheless finite. As such, transmission of the information is often accomplished in a cascade, where the state propagates cell by cell along the path. Thus, the issue of information transfer is essentially the interaction between the adjacent cells. Our investigation devised two approaches that can realize the crucial duplication (COPY) and inversion (NOT) operations of the upstream spin state in each of the cascading stages with a relatively simple control and layout arrangement. The first approach relies on the spin polarized current through the graphene channel, while the other takes advantage of the exchange

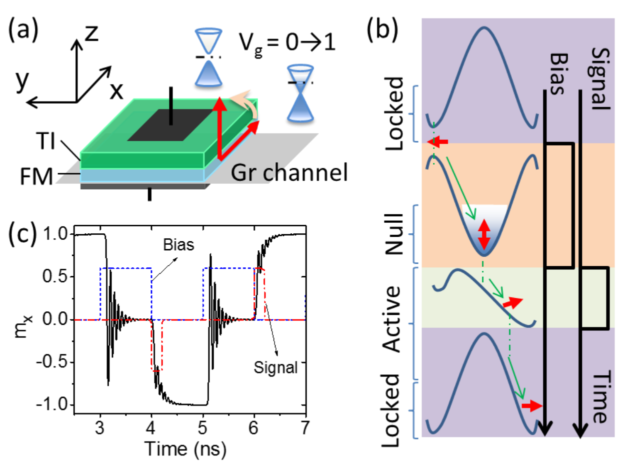

Figure 2: (a) Basic component (cell) of the proposed spin logic platform that consists of a two-layer structure of TI and FM plus the control gates. While not shown explicitly, top and bottom gate electrodes are separated from the active region by thin dielectrics. (b) Schematic illustration of the Bennett clocking scheme. The arrows indicate the evolution of the magnetization in ideal conditions. After relaxation, the magnetization is locked to a stable state along the easy axis. (c) Snapshots of magnetization evolution for 180° switches with Bennett clocking in the time domain (represented by m_x). Bias on the TI gate and signal pulses through the channel are indicated by the dashed blue and red lines.

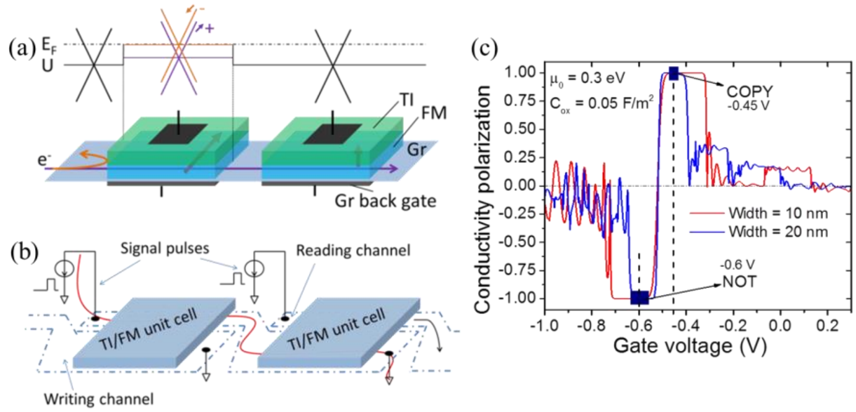

Figure 3: (a) Spin information transfer between the cells via the spin polarized current. (b) Asymmetrically patterned Read and Write channels to prevent the information backflow. (c) Interconnect conductivity (or channel current) polarization, demonstrating COPY and NOT via the back gate bias.

coupling between two magnets mediated by graphene electrons without involving the current flow.

In the approach based on the spin polarized current, the back gate bias is used to tune the spin dependent barrier in the graphene channel that is induced by the surface exchange interaction with the proximate magnet, selectively depleting the carriers of a specific spin state. Hence, the electrical bias determines the spin state of the transmitted signal in the interconnect [Fig. 3(a)]. The feasibility of this back gate function was examined by applying the Landauer-Büttiker formulism for carrier transport [Fig. 3(c)]. By taking advantage of large quantization energies in the narrow channels, the result demonstrated that the interconnect current can be made nearly 100% spin polarized even at room temperature – either parallel or antiparallel to that of the cell in the upstream. Accordingly, both functions COPY and NOT can be performed reliably with a sufficiently large bias window as required in the information transfer between two cells. The problem of possible back-propagation could be dealt with by a cascade structure with separately asymmetric read/write channels [Fig. 3(b)]. The energy consumption for each COPY or NOT operation was estimated to be of the order of femto-joules that is dominated by the Joule heating from the signal current.

A second, currentless mechanism of spin information transfer was also investigated by utilizing the exchange interaction mediated by the carriers in the graphene channel (Fig. 4). This mechanism is essentially analogous to the spin diffusion process albeit with an additional control. For instance, spin polarized electrons induced by the upstream cell (#1) diffuses to the target cell (#2) with the help of back gate biases [see "U" in Fig 4(a)]. The parallel/anti-parallel alignment can be determined by adjusting the length of the control magnet in the middle [Fig. 4(b)]. Our calculation clearly indicated that the carrier mediated mechanism can indeed induce a sufficiently large effective magnetic field at the target cell (over 1000 oe) leading to reliable magnetization switches. Furthermore, the estimate for energy consumption per single switching operation yielded a value as low as a few atto-joules, approximately two orders of magnitude smaller than the approach relying on the spin polarized current. The proposed currentless scheme may prove to be a ground-breaking alternative to the present state of the art. However, it still

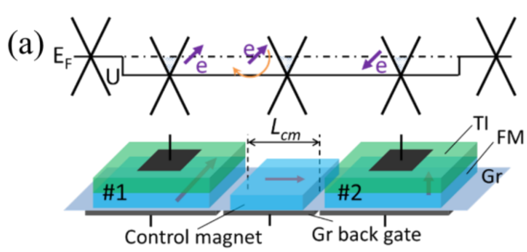

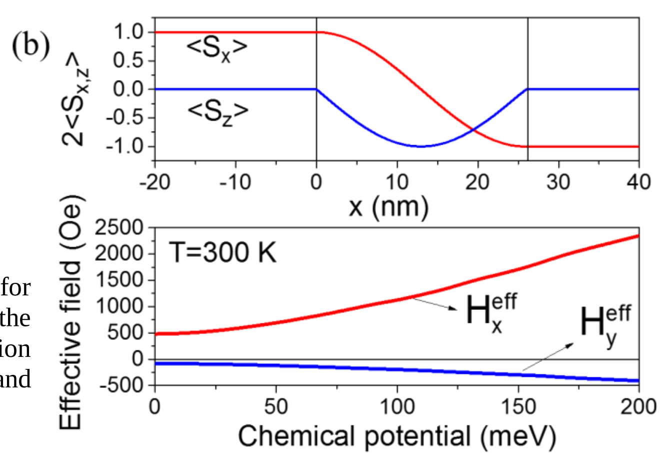

Figure 4: (a) Proposed currentless spin transfer for logic NOT. The design performs COPY without the control magnet. (b) Corresponding spin polarization vs. location in the channel with L_{cm}=26 nm (top) and effective magnetic field at cell #2 (bottom).

requires a more comprehensive analysis to fully verify the feasibility under realistic device/circuit layout conditions.

Once the elemental cell and the cell-to-cell COPY and NOT operations are established, the rest of the Boolean logic can be built on the spin logic platform with majority gates. As an example of the logic circuit implementation, the one-bit full adder was designed by utilizing the operating scheme based on the spin polarized current (see Fig. 3). A fully coupled device-circuit simulation method was developed to test the performance. The calculation results clearly illustrated the successful adder operation accurately following the desired truth table/Boolean logic, with the estimated energy consumption of approx. 15 fJ while maintaining the error rate below 10^{-6} for each switching operation. This energy requirement can be reduced significantly, perhaps as low as tens of atto-joules when the currentless approach is fully developed. The proposed spin logic platform based on the nanomagnet-Dirac fermion system appears very promising at least on paper.

(b) Nonlinear magnetization dynamics via a surface electrical current:

When an electrical current flows in the TI surface region interfaced with a magnetic material, the resulting natural spin polarization modulates the magnetization by tilting it toward the direction of the effective field as discussed above [sub-section (a)]. However, this is not the full story and the converse possibility must also be considered as the interaction is mutually dependent; namely, the reoriented magnetization self-consistently affects the TI surface current (both the intensity and spin polarization) through the electronic band modification. The resulting effective magnetic field and the associated magnetization dynamics are highly nonlinear, whereas the studies in the literature had examined only one aspect of the phenomenon (i.e., the linear regime). By developing a self-consistent theoretical treatment, we comprehensively analyzed the system response to an applied DC voltage (x direction). To obtain an accurate solution for the coupled system, it was assumed initially that the driving current (namely, J_x) can be described by coherent tunneling through the effective barrier on the TI surface which is formed by the magnet-induced band modification. The resulting magnetic response was mapped on the voltage-damping parameter space (Fig. 5). This diagram illustrates five distinct operation regimes, three (ii-iv) of which were previously unidentified; i.e., (i) slight deviation in the magnetization direction to align with the shifted stable position in a weak effective field; (ii) magnetization reversal (of 180°); (iii) several flip-flops followed by relaxation to a random final state; (iv) auto-oscillations (AO) between the +x and –x alignments; and (v) magnetization alignment along the y direction (i.e., the direction of the effective exchange field). All of these dynamical responses were accompanied by the strong anomalous Hall effect that enables electrical detection of the magnetic state as well. Time reversal symmetry imposes immutability under simultaneous reversal of initial magnetization and applied bias polarization. In the case when only one of these two factors reverses, the magnetization response maintained a similar bifurcation behavior but with different the threshold conditions (i.e., the phase boundaries), as shown by the red dashed lines in the figure.

Following the initial analysis based on the coherent tunneling model, the investigation was extended to more realistic conditions. In the non-coherent cases, on the other hand, a fully self-consistent treatment

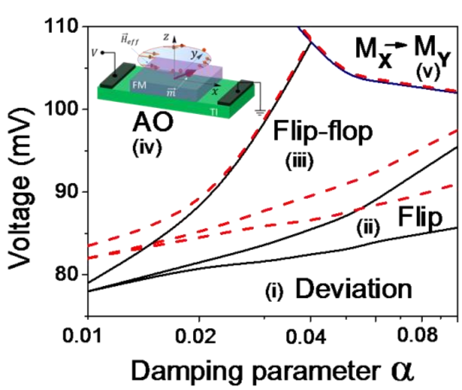

Figure 5: Self-consistent bifurcation behavior of magnetization dynamics induced by the TI surface current under coherent transport conditions. The insert shows the schematic structure that comprises a dielectric FM placed on top of a TI. Five dynamical phases are identified as a function of the driving voltage and the damping parameter strength. The red dashed lines illustrate a similar diagram when the input current/voltage is reversed (or the choice of $M_x < 0$ instead of $M_x > 0$ as the initial state). Coherent tunneling transport is assumed in the region of the TI capped by the FM.

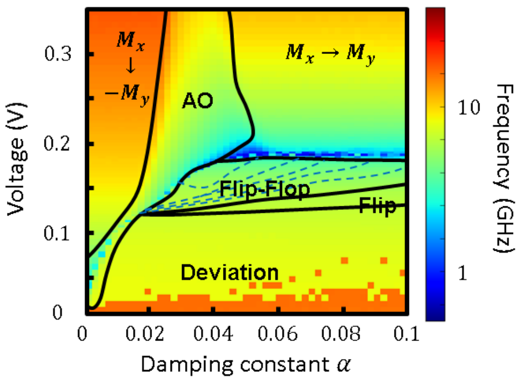

Figure 6: Magnetization dynamics mapped on the electrical bias (V)–Gilbert damping constant (α) parameter space. The diffusive transport is assumed for the TI surface electrons. The solid lines separate the different dynamical regimes, while the dashed lines in the flip-flop region indicate the smeared nature of the boundaries between the two final states (+x or −x) after the precession. The background color provides the corresponding frequency of the magnetization rotation. AO stands for auto (or sustained) oscillations.

is not possible at the moment due to a number of unknowns. As a result, an empirical approach was adopted based on the experimental and theoretical findings available in the literature concerning the anomalous Hall current, which turned out to be very crucial for the nonlinear magnetization dynamics. Figure 6 summarizes the obtained simulation results when the diffusive transport was assumed in the interface region. A key finding is that an entire range of the responses, such as reversal and auto-oscillations (with the frequencies in the GHz), are possible, even for diffusive cases, by simply adjusting the material and excitation conditions. One unexpected behavior is the possibility to anti-align the magnetization with respect to the effective field of the driving current. In other words, the magnetization may end up with the –y orientation even though the driving current induces a field along the +y axis via spin-momentum interlock. This scenario happens when the anomalous Hall effect becomes very pronounced and the resulting anti-damping effect dominates over the Gilbert damping term, which may turn out to be an artificial case. We have also examined the ballistic but incoherent case. The analysis revealed that the magnetization dynamics remain very similar to the diffusive case; except that the required voltages are now smaller due to the negligible resistance (thus, potential drop) in the channel. Compared with the previously discussed coherent transport (Fig. 5), the overall picture is again very consistent. Our investigation clearly indicated that the desired magnetic behaviors such as reversal and persistent oscillation can be achieved under broad regimes of TI surface electron transport with a simple DC electrical control. With a minimal energy requirement as low as tens of atto-joules, the proposed mechanism offers an efficient alternative to the spin transfer torque or spin-Hall based approaches for potential magnetic memory/logic. Note that this estimate did not consider the effect of thermal fluctuations in contrast to those cited in sub-section (a). The impact of the thermal noise on the nonlinear dynamical responses still remains an open question.

C. Multifunctional Current Modulation

(a) Quasi-optical transport of Dirac electrons:

We exploited the possibility of electron wave guiding on the surface of a TI in combination with a patterned layer of magnetic material. The electronic band modification induced by the symmetry-breaking exchange interaction at the TI-magnet interface can define the path of electron propagation in analogy to the optical fiber for photons (as the band mismatch amounts to an effective barrier). Numerical simulations based on the finite difference time domain (FDTD) method illustrated the guiding efficiency much higher than that in the waveguide formed by an electrostatic potential barrier such as p-n junctions. Further, the results indicated effective flux control and beam steering that can be realized by altering the magnetization/spin texture of the magnetic materials. These enable two key extensions of the concept whose functions are essential for active modulation of electron propagation. The first investigated structure was a waveguide defined by a ferromagnetic strip (FM), a segment of which can switch its magnetization direction [See Fig. 7(a)]. One can imagine that a 90° rotation in the control magnet either in the plane or out of the plane (thus, creating a misalignment with the channel) could block electron transmission through the region. The electron flow is restored once the "valve" is aligned with the main

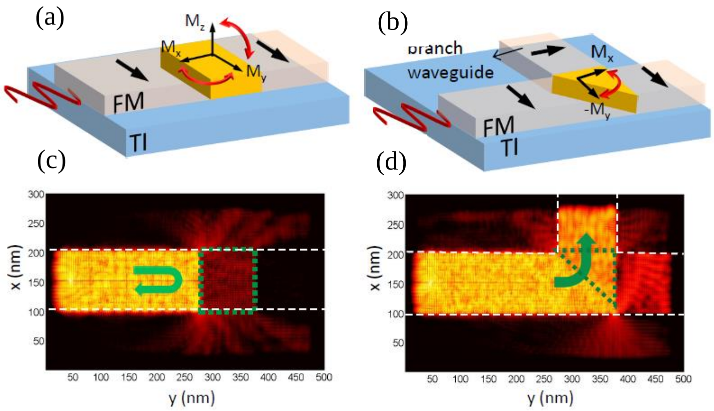

Figure 7: (a) Proposed electron wave guide with the flux ON/OFF switch. The magnetization direction of the middle piece (the yellow segment) is assumed to make 90° turn. (b) Proposed electron wave steering with the magnetization switching in the triangular shape region. (c,d) FDTD calculation of electron wave propagation in (a,b), respectively. The desired functions are demonstrated.

channel. Similarly, steering the electron beam into different directions can also be envisioned. For the latter, Fig. 7(b) shows a structure, where the main waveguide is connected with a second branch along the y direction through a triangular shape control region. By aligning the valve with either of the channels, the electrons may be made propagating along the main waveguide or diverted into the branch after rounding a 90° corner. A subsequent simulation based on the FDTD method demonstrated that both functions are indeed distinct possibilities as desired. Particularly appealing is the low leakage in the flux control. On other hand, it is somewhat larger for electron beam steering as a small portion continues its passage in the main waveguide instead of turning the corner. An additional barrier may be needed to further curtail the leakage.

This concept of electron wave guiding on the surface of a TI (with a patterned magnetic layer) was further examined to develop detailed understanding for potential device applications. In particular, the quasi-optical dynamics was examined analytically in terms of incident energy and angle, which was followed by the FDTD simulations for numerical verification (Fig. 8). A couple of features were apparent. First, the transmission is asymmetric around k_x=0 [i.e., the dependence on the electron incident direction; see Figs. 8(c,e,g) vs. Figs. 8(d,f,h)]. Second, a critical angle can be defined for each injection based on the injection energy (E) and the size of the effective barrier induced by the magnetic interaction (G_0), below which no transmission is allowed. This criterion clearly explains why the case of $E < \frac{1}{2}G_0$ shows no transmission [Figs. 8(a,b)], while the range extends to the negative angle (i.e., the incidence from the left)

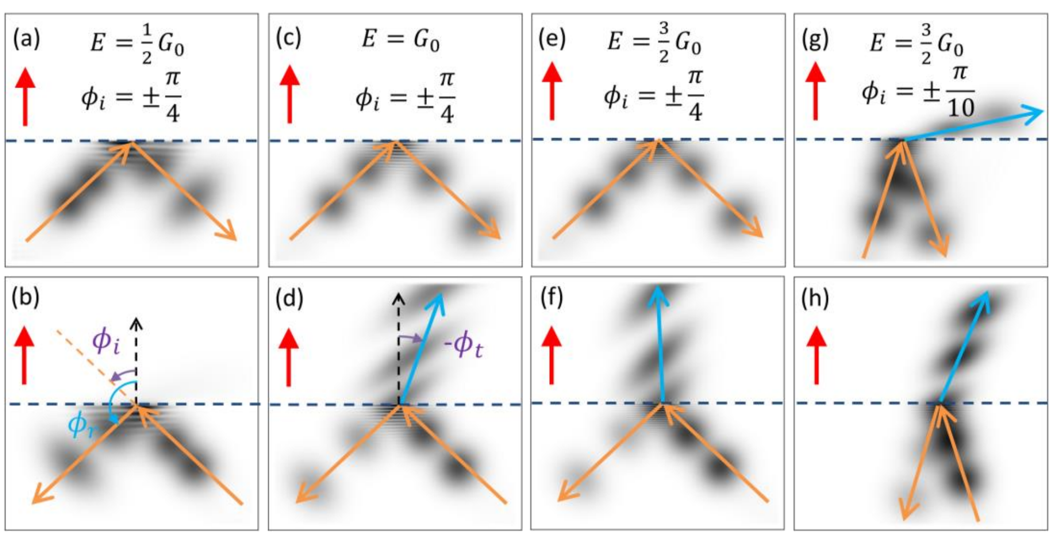

Figure 8: FDTD simulations of a Gaussian wavepacket incident to the magnetically induced junction (a,c,e,g) from the left and (b,d,f,h) from the right with various electron energies and angles. The block arrow (red) denotes the orientation of the magnetization along the +y direction. The junction is located at y=0.

once E > G_0 [see, for example, Fig. 8(g)]. When the magnetization at the junction switches to the –y direction (i.e., downward), the characteristic features are maintained except the π phase difference. An interesting consequence of this directional transmission is the generation of an anomalous Hall current. Even when the electrons are injected toward the boundary (at y=0) with a balanced distribution in the $+k_x$ and $-k_x$ space, the leftward moving electrons (i.e., $k_x < 0$) experience preferred transmission as discussed above [see Figs. 8(c,e,g) vs. Figs. 8(d,f,h)]. This also means an equal amount of the x-directional flux in the reflected electrons since the conservation rule must be satisfied at the junction. Hence, the applied bias or y-field induces an electron flow along the transverse x-axis at the junction boundary. Accessible by the standard Hall measurements, it offers a straightforward means to experimentally validate the predicted quasi-optical phenomenon on the TI surface.

(b) Magnetoelectric transistors with steep subthreshold slope:

Building on the possibility of electron wave guiding discussed above, we proposed and explored a transistor-like application mimicking the FET operation (i.e., gate controlled channel flux control). The device consists of a magnetically patterned channel and a magneto-electric (ME) valve (or gate) unit [Fig. 9(a)]. The ME unit is designed such that the magnetization rotates between the y and z directions according to the applied gate bias [See Fig. 7(a) as well]. Along the guided channel, the exchange potential induced by $m_y = -1$ (as shown) causes the band structure mismatch across the boundaries and confines electrons within the channel [Fig. 9(b); top panel]. When the valve is magnetized along the y direction (i.e., collinear to that of the channel region), the electrons injected from the source propagate freely to the drain, composing the ON state. On the other hand, the electron flow is severely restricted by formation of the barrier once the valve magnetization is switched 90° to the OFF position [Fig. 9(b); bottom panel]; see Fig. 9(c) for the corresponding conductance variation mapped on the magnetization space. The time resolved switching behavior was investigated by coupling the magnetization dynamics simulations with electron transport modeling. For initial demonstration of the concept, the 90° rotation of the magnetization was treated by considering the effective magnetic anisotropy of the TI/magnet structure controlled by the Fermi level [see also the discussion in sub-section B(a) for this mechanism between the in-plane and cross-plane orientations]. From the result [Fig. 9(d)], distinctive switching behaviors with a sizable ON/OFF current ratio can be clearly identified following the gate voltage variation.

Subsequently, the investigation was extended to a detailed analysis of the device performance including elementary logic functions. The intended advantage is that the applied gate bias modulates not only the electrostatic potential in the channel but also the TI surface state band structure itself, leading to a more drastic response in the drain current than that of conventional FETs. The calculation based on the non-equilibrium Green's function method and the LLG magnetization simulation indeed illustrated the I_D-V_G curve with the desired sharp ON/OFF characteristics [Fig. 10(a)]. The switching behaviors were identified

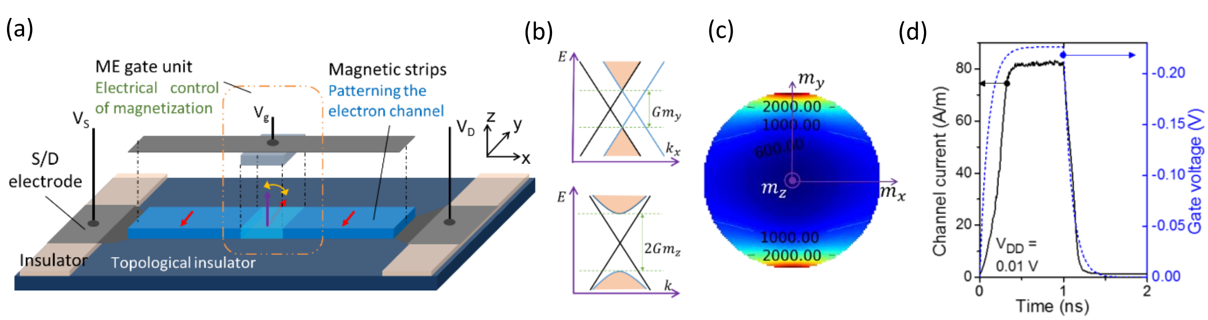

Figure 9: (a) Proposed TI based magneto-electric transistor. The gate region extended beyond the ME unit is optional. (b) Band structure mismatch across the magnetic boundary. The exchange potential shifts the bands in the k-space (guiding) or opens a gap (blocking). Transmission only happens where the band structures across the boundary overlap (i.e., the colored region). (c) Channel conductance mapped on the m_x-m_y plane of the valve magnet ($60\times60\times2$ nm^2). The TI chemical potential is assumed to be at 0.05 eV. (d) Time resolved switching by a gate bias pulse for a typical transistor ON/OFF operation. The data is averaged over 100 stochastic simulations.

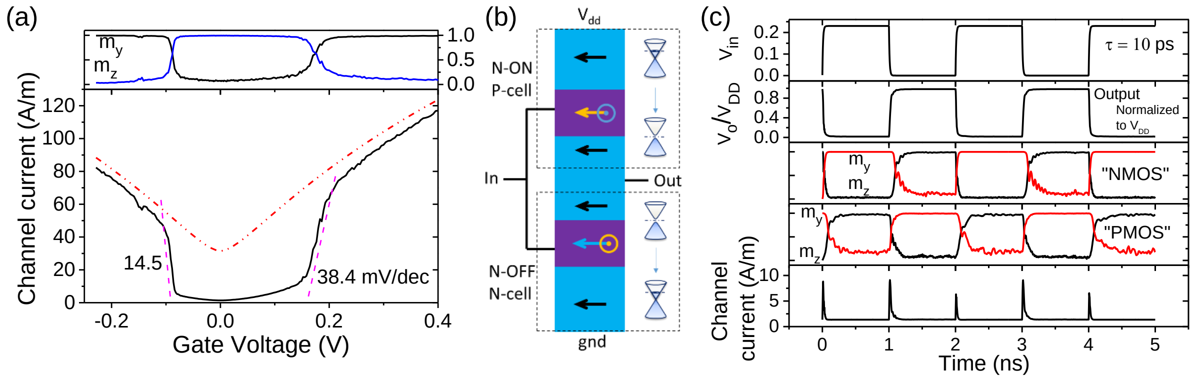

Figure 10: (a) Drain/channel current calculated as a function of the gate bias in the FET-like device. The corresponding change in the magnetization of the magnetic gate dielectric is also provided (top panel). The red dashed-dotted curve indicates the result when only the electrostatic control of the gate bias is considered. (b) A complementary inverter with one normally ON p-type and one normally OFF n-type devices. The purple blocks represent the switching magnets. (c) Simulated transient behavior of the inverter. From top to bottom, the panels show the input signal, output signal, n-device magnetization, p-device magnetization, and channel current, respectively. All figures are drawn with a channel supply voltage of 0.01 V.

on both the positive and negative sides (i.e., p-FET and n-FET) with the equivalent subthreshold slope as steep as 15 mV/decade. In comparison, the channel ON/OFF performance is much more gradual under the conventional gate control (see the red curve). The investigation also revealed that both the normally ON and normally OFF operations can be attained by proper adjustment of the doping density in the TI. Based on these results, the device and circuit possibilities were further examined. Shown in Fig. 10(b) is a proposed logic inverter constructed with one normally ON p-device and one normally OFF n-device. The simulated transient inverter performance [top two panels in Fig. 10(c)] clearly indicated that the output produces the desired signal in reference to the input. While the proposed device may have a limited ON/OFF ratio of around 100, the steep subthreshold slope offers a unique advantage for low power applications. Further optimization of the performance is expected by adopting a multiferroic heterostructure with a strong magnetoelectric effect in place of an ordinary magnetic insulator as the gate dielectric.